Solidification in developing pipe flows

Shih-Shan Wei and Selçuk I. Güçeri
Thermal Engineering and Advanced Manufacturing Group, Department of Mechanical Engineering, University of Delaware, Newark, DE 19716, USA

Received 29 January 1987 and accepted for publication in final form on 22 June 1987

A numerical solution is presented for the problem of transient freezing of laminar flows inside a circular pipe. Unlike other available solutions on similar subjects, the flow motion in the present study is determined as part of the solution where the fluid transport process is represented by the elliptic Navier-Stokes equations characterized by diffusion in the radial and axial directions. In the solid and liquid regions, thermal diffusion is accounted for in the axial direction as well as in the radial direction. The vorticity-stream function approach is used in the formulation of the flow problem. A Landau transformation is applied to map the variable-geometry physical domain into a fixed-geometry computational domain. A time-lag procedure is employed to treat the moving grids, and interpolation is used to determine the field variables at the new grid locations from those known at the old grid points. Three cases of flow motion are considered: flow with uniform velocity at the entrance, flow with fully developed profile at the entrance, and slug flow through the pipe. The position of the solid-liquid interface, the temperature distribution, heat flux at the walls, and the heat transfer coefficient at the interface have been calculated for prescribed and calculated velocity profiles. Differences in solidification rates for the three kinds of flow configurations demonstrate that the computed flow profiles show significantly different results from the slug flow case, demonstrating the need for accurate treatment of the flow field. The influences of the Reynolds and Stefan numbers on the solidification rate are also investigated. The accuracy of the present method is verified by comparing the results with the closest analytical solution using the case of a slug velocity profile through a pipe.

Keywords: developing flows; solidification; Landau transformation

Introduction

In many practical engineering problems the solidification of fluids in an internal pipe flow in the entrance region is of interest and importance. In some cases, such as in chilled-water air conditioning systems, water supply through pipes in a cold environment, and fluid flow in process industries, freezing of the fluids may be critical and potentially damaging. Also, in applications like casting, the cooling rate is one of the important factors in determining the microstructure of the final products.

One inherent difficulty in solving problems of this type is that the solid-liquid interface moves in time and is not known a priori. Another difficulty arises in determining the liquid flow through a continuously deforming domain. The effect of flow motion becomes particularly important when the thermal behavior of the fluid needs to be taken into account. Two of the earliest significant investigations on this subject were reported by Hirschberg[1] and Zerkle and Sunderland[2] for liquid solidification in a tube with the assumption of steady-state laminar flows. Later, Ozisik and Mulligan[3] presented a solution for transient freezing of laminar flows inside channels, assuming a constant wall temperature. The effects of convectively cooling boundary conditions were reported by Sadeghipour, Ozisik, and Mulligan[4]. Shibani and Ozisik[5,6] presented solutions for the freezing of turbulent, internal flows. A variational solution was obtained by Bilenas and Jiji[7] for the problem of axisymmetric fluid flow in tubes with surface solidification. The common simplifying assumptions in these studies are the prescribed velocity profiles, quasi-steady-state heat conduction in the solid region, and negligible axial conduction. Another assumption commonly made in the theoretical analysis of the solidification problem is that the solid-liquid interface is smooth and the flow cavity has a monotonically decreasing diameter. Instead, Gilpin[8,9] observed wavelike or cyclic variation in cross section along the axial direction of the tube. Gilpin found that ice-band spacing normalized by the pipe diameter is independent of the flow Reynolds number and can be correlated with the cooling ratio $\theta_c((T_m - T_w)/(T_o - T_m))$ for laminar and turbulent flows. Ice-formation phenomena for water flow between two horizontal parallel plates were investigated by Seki, Fukusako, and Younan[10]. Smooth ice-formation types and transition ice-formation types were observed, both occurring for $\mathrm{Re}/\theta_c^{0.741} \gtrless 10^4$, respectively. Cheung and Epstein[11] collected and reviewed the important results of the work on the solidification and melting in fluid flow in the literature up to 1982.

The finite difference methods and the vorticity–stream function formulation for the flow motion supply a means of solving phase-change problems numerically rather than analytically. Barakat and Clark[12] successfully applied these methods to solve a problem of two-dimensional transient laminar natural convection. Kroeger and Ostrach[13] used this approach to solve phase-change problems, including convection effects in the liquid region. Yim *et al.*[14] presented experimental studies as well as some comparison with a simplistic quasi-steady-melting model and Petrie *et al.*[15] reported a similar study for two-phase flows. Thomason and Mulligan[16] and Thomason, Mulligan, and Everhart[17] experimentally investigated the flow instability and pressure drop during the freezing of turbulent internal pipe flows. Several studies employed transformation techniques to analyze the multidimensional phase-change problem by mapping the physical domain into a simpler computational domain[18-21]. Recently, boundary-fitted coordinate systems using numerically generated grids have been applied to analyze problems that have solid-liquid interfaces of complex shapes[22-24].

Even though there have been many studies on the subject of the solidification of internal channel flows, the complete governing equations which really represent the solidification process have not been solved. In the present investigation, a finite difference algorithm has been developed to solve the problem of transient freezing of a two-dimensional forced laminar flow inside a pipe using a Landau transformation. The assumptions that are frequently made, such as negligible axial conduction and quasi-steady-state heat conduction in the solid region, have been removed, and the flow motion is determined as part of the solution. The solid-liquid interface is assumed to be smooth and monotonically decreasing along the axial direction. This assumption is validated by considering that the solidification occurs in the inlet region. The cooling temperature ratio θ_c in the present analysis ranges from 0.5 to 2.5, which reflects the ratio of ice-band spacing to pipe diameter to be larger than 15 from Gilpin's correlation[9]. However, the ratio of pipe length to pipe diameter is 10, which implies that less than one ice-band is considered in the present study. The comparison between the present numerical solution obtained from the complete governing equations for the solidification process and other available analytical solutions obtained from the simplified governing equations is used to establish the validity of the slug flow assumptions made in the literature.

Problem formulation

The transient freezing of an axisymmetrical flow inside a straight circular pipe is considered. Initially, the fluid inside the pipe is assumed to be at rest with its temperature at the freezing point, T_m. The fluid then starts flowing along the axial direction which is accompanied by a step reduction of the wall temperature T_w down to a value below the freezing point. The flow temperature at pipe inlet is T_o, which is higher than the freezing point. A solidified region quickly forms over the inside surface of the pipe wall and grows toward the centerline. Figure 1 illustrates the geometry and the general nomenclature for the problem. The flow is assumed to be axisymmetrical, laminar, and incompressible. Furthermore, it is assumed that the fluid has a well-defined, distinct freezing point, and its density remains unchanged during solidification.

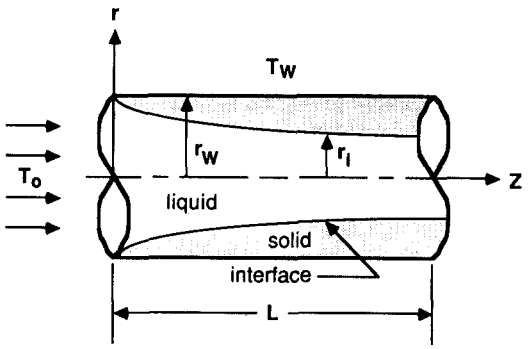

Figure 1 The nomenclature and the schematic description for solidification in developing pipe flows

The equations governing the present problem are those resulting from conservation principles and can be expressed as follows:

Solid region

$$\frac{\partial^2 T_s}{\partial z^2}+\frac{1}{r}\frac{\partial}{\partial r}\left(r\frac{\partial T_s}{\partial r}\right)=\frac{1}{\alpha_s}\frac{\partial T_s}{\partial t} \tag{1}$$

Notation

c_p Specific heat
h Local heat transfer coefficient, $-k_l(\partial T_l/\partial r)_i/(T_b-T_m)$
H Dimensionless local heat transfer coefficient, $2r_w h/k_l$
k Thermal conductivity
K Dimensionless thermal conductivity, $k(T_m-T_w)/\alpha_l\rho_l\lambda$
L Pipe length
p Fluid pressure
P Dimensionless pressure, $pr_w^2/\rho_l\alpha_l^2\mathrm{Pr}$
Pr Prandtl number of the liquid, ν_l/α_l
q Local heat flux, $-k_s(\partial T_s/\partial r)$
Q Dimensionless heat flux, $qr_w/k_l(T_o-T_m)$
r Radial coordinate
R Dimensionless radial coordinate in the liquid region, r/r_i
R^* Dimensionless radial coordinate in the solid region, $(R-1)/(1/R_i-1)$
R_i Dimensionless radial location of the interface, r_i/r_w
Re Reynolds number, $2u_b r_w/\nu$
Sf Stefan number, $c_{p_l}(T_m-T_w)/\lambda$
t Time
T Temperature
T_b Bulk mean temperature
u_c Velocity at the centerline
U_c Dimensionless centerline velocity, $r_w u_c/\alpha_l$
u_b Mean velocity at the entrance
u_r Radial velocity
U_r Dimensionless radial velocity, $r_w u_r/\alpha_l$
u_z Axial velocity
U_Z Dimensionless axial velocity, $r_w u_z/\alpha_l$
z Axial coordinate
Z Dimensionless axial coordinate, z/r_w

Greek symbols
α Thermal diffusivity
θ Dimensionless temperature, $(T-T_m)/(T_m-T_w)$
θ_c Cooling temperature ratio, $(T_m-T_w)/(T_o-T_m)$
λ Latent heat
μ Viscosity
ρ Density
τ Dimensionless time, $t\alpha_l\mathrm{Sf}/r_w^2$
ψ Stream function
Ψ Dimensionless stream function, $\psi/\alpha_l r_i$
ω Vorticity, $\partial u_z/\partial r-\partial u_r/\partial z$
Ω Modified dimensionless vorticity, $\omega r_i r_w/\alpha_l R$

Subscripts
i Solid-liquid interface
l Liquid zone
m Melting/freezing
o Pipe inlet
s Solid zone
w Pipe wall

Superscript
n Computational time level

Liquid region

$$\frac{\partial u_z}{\partial z}+\frac{1}{r}\frac{\partial}{\partial r}(ru_r)=0 \tag{2}$$

$$\rho_l\left(\frac{\partial u_r}{\partial t}+u_r\frac{\partial u_r}{\partial r}+u_z\frac{\partial u_r}{\partial z}\right)=-\frac{\partial p}{\partial r}+\mu\left(\frac{\partial^2 u_r}{\partial r^2}+\frac{1}{r}\frac{\partial u_r}{\partial r}-\frac{u_r}{r^2}+\frac{\partial^2 u_r}{\partial z^2}\right) \tag{3}$$

$$\rho_l\left(\frac{\partial u_z}{\partial t}+u_r\frac{\partial u_z}{\partial r}+u_z\frac{\partial u_z}{\partial z}\right)=-\frac{\partial p}{\partial z}+\mu\left(\frac{\partial^2 u_z}{\partial r^2}+\frac{1}{r}\frac{\partial u_z}{\partial r}+\frac{\partial^2 u_z}{\partial z^2}\right) \tag{4}$$

$$\frac{\partial T_l}{\partial t}+u_r\frac{\partial T_l}{\partial r}+u_z\frac{\partial T_l}{\partial z}=\alpha_l\left(\frac{\partial^2 T_l}{\partial r^2}+\frac{1}{r}\frac{\partial T_l}{\partial r}+\frac{\partial^2 T_l}{\partial z^2}\right) \tag{5}$$

At interface

$$\left(1+\left(\frac{\partial r_i}{\partial z}\right)^2\right)\left(k_s\frac{\partial T_s}{\partial r}-k_l\frac{\partial T_l}{\partial r}\right)=\rho_l\lambda\frac{\partial r_i}{\partial t} \tag{6}$$

In order to avoid performing calculations in the transient and irregularly shaped domains, we apply the Landau transformation twice. The first Landau transformation is applied to the governing equations through a change of variables and nondimensionalization by defining

$$R\equiv r/r_i \tag{7a}$$

$$R_i\equiv r_i/r_w \tag{7b}$$

Based on common observation, it is assumed that the rate of change of the radial position of the interface with respect to the axial direction is small. This assumption can be validated by observing the transient development of the ice structure in a pipe reported in Ref. 9. This assumption of negligible interface slope, $\partial r_i/\partial z$ reduces the complexity and length of the transformed derivatives, subsequently giving

$$\frac{\partial}{\partial r}=\frac{1}{r_i}\frac{\partial}{\partial R},\quad \frac{\partial}{\partial z}=\frac{1}{r_w}\frac{\partial}{\partial z},\quad \frac{\partial}{\partial t}=\frac{\alpha_l \mathrm{Sf}}{r_w^2}\frac{\partial}{\partial \tau}$$
$$\frac{\partial^2}{\partial r^2}=\frac{1}{r_i^2}\frac{\partial^2}{\partial R^2},\quad \frac{\partial^2}{\partial z^2}=\frac{1}{r_w^2}\frac{\partial^2}{\partial Z^2} \tag{8}$$

It is necessary to explain more carefully the transformation of the time derivative. Since the solid-liquid interface location r_i is time-dependent in the transient freezing problem, the time derivative should be formally transformed into the expression

$$\frac{\partial}{\partial t}=\frac{\partial \tau}{\partial t}\frac{\partial}{\partial \tau}+\frac{\partial R}{\partial t}\frac{\partial}{\partial R}=\frac{\alpha_l \mathrm{Sf}}{r_w^2}\left[\frac{\partial}{\partial \tau}-\frac{R}{R_i}\frac{\partial R_i}{\partial \tau}\frac{\partial}{\partial R}\right] \tag{9}$$

In the treatment of a moving-grid-type problem, there are basically two approaches: One is to consider the dependence of the variables on both time and space. This leads to the second term of the type $(\partial R/\partial t)(\partial/\partial R)$. This term can be seen as a "velocity" quantity indicating the velocity of the coordinate points, as treated by Saitoh and Hirose[20]. A second approach, which is used in the present work, is to consider the "pseudo steady-state" problem and assume that during each time step the solution domain remains unchanged. The validity of this assumption can be further verified by noting that the second term is an order of magnitude less than the first term. Although the first procedure may appear to provide a more accurate solution, the numerical evaluation of the derivatives contains substantial errors. On the other hand, the second approach becomes more straightforward and accurate, particularly for slowly deforming domains of the type considered in the present work. This approach has been utilized by Sparrow, Patankar, and Ramadhyani[18] in their investigation of the effects of natural convection on the melting process.

After the first transformation process, the entire physical domain is mapped onto a new one, where the liquid region is rectangular; i.e., $0\leq Z\leq L/r_w$, $0\leq R\leq 1$, and the solid-liquid interface is always maintained at $R=1$. However, the solid region after the first transformation is still neither time-independent nor rectangular; i.e., $1\leq R\leq 1/R_i$. A second Landau transformation is employed to immobilize the domain of the solid region that has been obtained by the first transformation process. This is accomplished by defining a new transformation variable

$$R^*=\frac{R-1}{1/R_i-1} \tag{10}$$

which yields

$$\frac{\partial}{\partial R}=\frac{R_i}{1-R_i}\frac{\partial}{\partial R^*} \tag{11}$$

In the present study, a vorticity–stream function formulation is used to represent the fluid motion. The resulting governing equations in terms of dimensionless variables are as follows:

Solid region $(0\leq R^*\leq 1,\ 0\leq Z\leq L/r_w)$

$$\frac{\alpha_l \mathrm{Sf}}{\alpha_s}\frac{\partial \theta_s}{\partial \tau}=\frac{\partial^2\theta_s}{\partial Z^2}+\frac{1}{R^*(1-R_i)+R_i}\frac{1}{1-R_i}\frac{\partial \theta_s}{\partial R^*}+\frac{1}{(1-R_i)^2}\frac{\partial^2\theta_s}{\partial R^{*2}} \tag{12}$$

Liquid region $(0\leq R\leq 1,\ 0\leq Z\leq L/r_w)$

$$\mathrm{Sf}\frac{\partial \Omega}{\partial \tau}+\frac{U_r}{R_i}\frac{\partial \Omega}{\partial R}+U_z\frac{\partial \Omega}{\partial Z}=\mathrm{Pr}\left(\frac{1}{R_i^2}\frac{\partial^2\Omega}{\partial R^2}+\frac{3}{R_i^2 R}\frac{\partial \Omega}{\partial R}+\frac{\partial^2\Omega}{\partial Z^2}\right) \tag{13}$$

$$R^2\Omega=\frac{1}{R_i}\frac{\partial^2\Psi}{\partial R^2}-\frac{1}{R_i R}\frac{\partial \Psi}{\partial R}+R_i\frac{\partial^2\Psi}{\partial Z^2} \tag{14}$$

$$\mathrm{Sf}\frac{\partial \theta_l}{\partial \tau}+\frac{1}{R_i}U_r\frac{\partial \theta_l}{\partial R}+U_z\frac{\partial \theta_l}{\partial Z}=\frac{1}{R_i^2}\frac{\partial^2\theta_l}{\partial R^2}+\frac{1}{R_i^2}\frac{1}{R}\frac{\partial \theta_l}{\partial R}+\frac{\partial^2\theta_l}{\partial Z^2} \tag{15}$$

where

$$U_z=\frac{1}{R_i R}\frac{\partial \Psi}{\partial R},\qquad U_R=-\frac{1}{R}\frac{\partial \Psi}{\partial Z} \tag{16}$$

$$\Omega=\frac{1}{R}\left(\frac{\partial U_z}{\partial R}-R_i\frac{\partial U_r}{\partial Z}\right) \tag{17}$$

Solid-liquid interface $(R=1,\ R^*=0,\ 0\leq Z\leq L/r_w)$

$$R_i \mathrm{Sf}\frac{\partial R_i}{\partial \tau}=\left(K_s\frac{R_i}{1-R_i}\frac{\partial \theta_s}{\partial R^*}-K_l\frac{\partial \theta_l}{\partial R}\right) \tag{18}$$

A modified form of the vorticity variable as shown above[7] is used for improved formulation and computational advantage.

Boundary conditions

Due to the elliptic nature of the conservation equations, the boundary conditions for all the field variables have to be specified along the entire boundary enclosing the solution domains. At the inlet of the pipe, the stream function distribution is calculated from the specified inlet fluid velocity profile for which two cases (i.e., slug and parabolic profiles) are considered. At the outlet, the gradient of the stream function in the axial direction is assumed to be zero; i.e., the streamlines are assumed to be perpendicular to the exit plane of the pipe. This boundary condition frequently appears in the literature[25] and implies that the flow is almost fully developed at the exit. Even though the fully developed condition may not be achieved at the exit of the channel, this zero-gradient boundary condition offers sufficient flexibility for the flow distribution. Furthermore, it is intuitively very accurate for narrow channels of the type

considered in the present study and has negligible influence on the upstream portion of the flow. At the interface, the condition of no flow in the direction perpendicular to the interface is applied, which we can justify by noting that for the problem under consideration the progress of the solidification interface is much slower by comparison with the residence time for the fluid flow. This would not be accurate for flows subject to very rapid solidification. On the centerline, the stream function remains constant due to axisymmetry.

The vorticity boundary conditions are derived from velocity distributions at the inlet and are zero on the centerline by the axisymmetrical flow consideration. As for the stream function, the vorticity is assumed to have zero gradient at the exit. At the interface,

$$\Omega(Z,1,\tau)=\frac{1}{R}\frac{\partial U_z}{\partial R}=\frac{1}{R_i}\frac{\partial^2\Psi}{\partial R^2} \tag{19}$$

which can be obtained by using a Taylor series expansion[25]. The fluid is assumed to have a uniform temperature distribution at the inlet; at the outlet the temperature gradient along the flow direction is taken to be negligible, indicating that the convective effects are taken to be much more dominant than the diffusion of heat. The axial conduction at the pipe exit in the solid region is also assumed negligible. This can be justified by noting that the radial dimension is much shorter than the overall length of the pipe section considered in this study. Thus, the major thermal gradients that cause solidification occur solely in the radial direction as the flow develops. Therefore the temperature distribution in the solid region at the exit zone is almost one-dimensional as the solidification front becomes increasingly parallel to the axis. This is also apparent from Figures 2, 7, and 8 when the radial and axial directions are properly scaled. The solid-liquid interface is assumed to be isothermal and has the value of the melting point. On the centerline, the axisymmetric boundary condition is applied. Summarizing, we have the following:

At the entrance:

$$\Psi(0,R,\tau)=U_cR_i(R^2/2-R^4/4)$$ for parabolic velocity at inlet (20)

$$\Psi(0,R,\tau)=\tfrac{1}{2}U_cR_iR^2$$ for slug velocity profile at inlet (21)

$$\Omega(0,R,\tau)=-2U_c$$ for parabolic velocity profile at inlet (22)

$$\Omega(0,R,\tau)=0$$ for slug velocity profile at inlet (23)

$$\theta_l(0,R,\tau)=\theta_0 \tag{24}$$

$$\theta_s(0,R,\tau)=\theta_0 \tag{25}$$

At the exit:

$$\frac{\partial\Psi(L,R,\tau)}{\partial Z}=\frac{\partial\Omega(L,R,\tau)}{\partial Z}=\frac{\partial\theta_l(L,R,\tau)}{\partial Z}=\frac{\partial\theta_s(L,R^*,\tau)}{\partial Z}=0 \tag{26}$$

Along the centerline:

$$\Psi(Z,0,\tau)=0 \tag{27}$$

$$\Omega(Z,0,\tau)=0 \tag{28}$$

$$\frac{\partial\theta_l(Z,0,\tau)}{\partial R}=0 \tag{29}$$

At the solid-liquid interface:

$$\Psi(Z,1,\tau)=\text{volumetric flow rate} \tag{30}$$

$$\Omega(Z,1,\tau)=\frac{2(\Psi_p-\Psi_w)}{R_i(\Delta R)^2} \tag{31}$$

where Ψ_p is the stream function value at the node in the fluid, which is one nodal distance ΔR away from the solid interface.

$$\theta_l(Z,1,\tau)=\theta_s(Z,0,\tau)=0 \tag{32}$$

The pipe surface is considered to be held at a constant temperature that is lower than the freezing point of the fluid, starting at the pipe entrance; thus

$$\theta_s(Z,1,\tau)=-1 \tag{33}$$

The above set describes the complete boundary conditions needed to solve the present problem.

Numerical procedure

An explicit finite difference method is adopted to solve the governing equations. The convective terms in Equations 13 and 15 are linearized by assuming that the velocity components U_r and U_z have the same values as they did at the previous time step. A first-order upwinding scheme is used to represent the convective terms, and second-order central differencing is used for the remaining derivative terms. For the terms $(1/R)(\partial\theta_l/\partial R)$ and $(1/R)(\partial\Psi/\partial R)$, a singularity occurs at $R=0$; this singularity is eliminated by taking the limit forms of these terms. In order to obtain satisfactory accuracy, the temperature gradient at the interface is evaluated by a second-order one-sided differencing in both the solid and liquid regions.

One of the main computational difficulties is the determination of the interface movement. To circumvent this problem, we use a time lag procedure, which assumes that the moving interface is stationary during a small time interval between the heat transfer and the progress of the interface. At each time step, the fluid motion is evaluated using Equations 13 and 14. After the flow field is obtained, the temperature distribution in both solid and liquid regions can be obtained by using Equations 12 and 15, respectively. The new position of the interface can thus be determined from Equation 18 as

$$R_i^{n+1}=R_i^n+\frac{\Delta\tau}{R_i\mathrm{Sf}}\left(K_s\frac{R_i}{1-R_i}\frac{\partial\theta_s}{\partial R^*}-K_l\frac{\partial\theta_l}{\partial R}\right) \tag{34}$$

An identical computation procedure can be employed again to yield all the variables and the interface location at the next time step, and so forth.

The result of the Landau transformation and the time-lag procedure is that the relationship between a given radius position in the physical domain and the transformed coordinates changes as the interface moves. Subsequently, a fixed point on the computational domain corresponds to different physical locations at two consecutive time steps. Thus, a reevaluation of the field variables after each time step is required. This is carried out by linear interpolation at all grid points except those which correspond to the newly solidified region. For these, the stream function and the vorticity are assumed to have their values at the interface, and the temperature is assumed to be at the freezing point. Furthermore, to fulfill both local and overall mass conservation, the interpolation for the velocity components is performed by differentiating the stream functions at the newly mapped points.

In order to keep the explicit finite-difference calculation stable, the time increment is evaluated before the computation at each time step. It can be seen that the explicit finite-difference expressions for the governing equations can be written in the form

$$\Pi_{I,J}^{n+1}=(A_{I,J}^n\Pi_{I-1,J}^n+B_{I,J}^n\Pi_{I+1,J}^n+C_{I,J}^n\Pi_{I,J-1}^n+D_{I,J}^n\Pi_{I,J+1}^n)\Delta\tau+(1-E_{I,J}^n\Delta\tau)\Pi_{I,J}^n \tag{35}$$

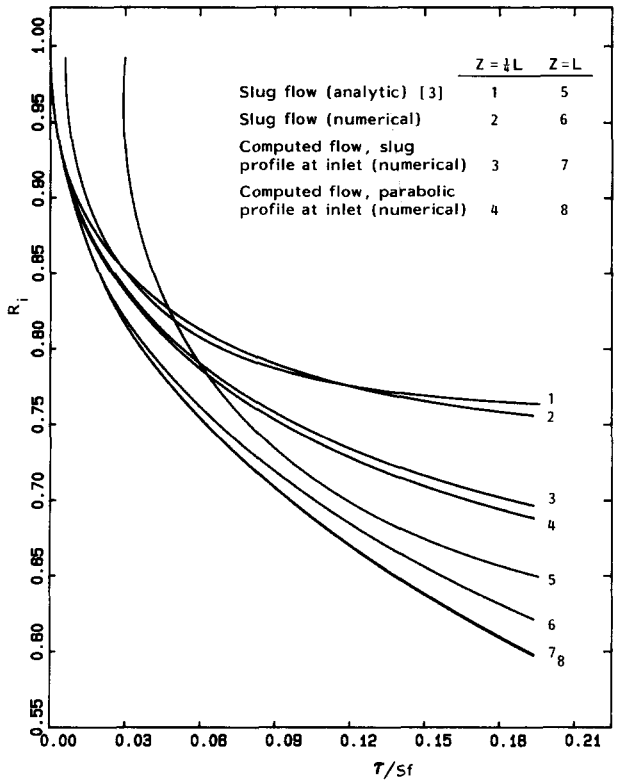

Figure 2 Variation of solidification front with time at selected axial locations for Sf=0.643, Pr=13.2, and Re=100

where Π can represent temperature or vorticity and A, B, C, D, and E are the coefficients evaluated from the field variables. Stability requires that the coefficients in front of Π be positive. Since A, B, C, D, and E are always positive, the stability criterion becomes

$$1 - E^n_{I,J}\Delta\tau \geqslant 0 \tag{36}$$

In the present problem, meshes of 21×10 in the solid region and 21×12 in the liquid region, in the axial and radial directions, respectively, have been used to generate the results. In the computational domains, the grids are evenly separated along each direction, which results in a uniform distribution of points in the axial direction and a skewed distribution in the radial direction of the physical domain. The grid independence study is carried out by doubling the grid number in the axial direction (i.e., meshes of 41×10 in the solid region and 41×12 in the liquid region). The reason for doubling the nodal points in the axial direction is that the nodal point distribution in the axial direction has much larger spacing than that in the radial direction. The solid-liquid interface positions derived using the doubled grid solution show no visible difference from those displayed in Figure 2.

Results and discussion

In order to generate results and perform comparative evaluation with results obtained by analytic methods and different nondimensional variables, the thermal and fluid properties close to those of water at 0°C are selected for computation. Sf = 0.643, Pr = 13.2, and Re = 100 are used in Figure 2 through Figure 6. The pipe length is 10 pipe diameters. The fluid motion is handled in two distinct ways. First, a slug velocity profile is assumed, which eliminates the need to compute the velocity field, and the value of the mean velocity is obtained from continuity. This case enables the results to be compared with analytical solutions to assess the accuracy in solving the moving-boundary problem. Furthermore, this case approximates turbulent flows with flatter velocity profiles. In the second group of computations, full expressions governing the fluid motion are considered which are referred to as the computed exact velocity solutions. In both of these cases, a constant mass flow rate of liquid through the entrance of the pipe is considered, which would indicate the necessity for providing a greater pressure difference to maintain the flow rate as the solidification progresses. This assumption, however, is not a limitation of the approach, and any time-dependent inlet velocity profile can be considered once it is specified or coupled with the pressure drop.

Figure 2 shows the transient behavior of the solid-liquid interface position at a quarter of the pipe distance from the inlet and at the end of the pipe. Included in this figure are the analytic results obtained by Ozisik and Mulligan[3] for a slug velocity profile through the pipe, numerical results for a slug flow, and numerical results for fluid flow with given velocity distributions at the entrance. The deviation between the analytic and numerical results for both slug flows can be attributed to the absence of axial conduction and the quasi-steady-state assumption for the solid phase in the analytic results, which have been accounted for in the present study. Figure 2 also reveals that the solidification rate is faster if exact velocity profiles are computed simultaneously rather than if a slug velocity profile through the pipe is used in the flow motion. This phenomenon can be explained in that the motion of fluid particles close to the solid zone move more slowly than those at the centerline for the computed flow field, reducing the thermal gradient at the liquid side of the interface. This also shows that for the computed flow field, the influence of the velocity profile at the entrance diminishes as the flow develops further downstream.

Figure 3 shows the temperature distribution as a function of the radius at a quarter of the pipe length from the inlet and at the end of the pipe. Closer examination of the results from analytic and numerical methods for the slug flows reveals that the influence of axial conduction on the temperature distribution is significant, especially at the downstream of the pipe. This also can explain the reason why the deviation between curve 5 and curve 6 is larger than that between curve 1 and curve 2 in Figure 2. Figure 4 displays the dimensionless local heat flux along the wall for the different kinds of velocity profiles. Plotted in Figure 5 is the dimensionless local heat transfer coefficient at interface over the range $Z = \frac{1}{20}L$ to $Z = L$. The heat flux and the heat transfer coefficient are determined by the temperature distribution. Figure 6 shows the calculated velocity profiles. The flow development can be noted by comparing the profiles for the case of $Z = \frac{1}{4}L$ and $Z = L$. This further justifies the gradient boundary conditions which are used for the flow variables.

Figure 7 depicts the effect of the Stefan number (Sf = 0.129, 0.386, and 0.643) on the location of the solid-liquid interface at the pipe exit as a function of the dimensionless time. A large Sf value indicates a small value of latent heat and/or a large freezing-to-wall temperature difference. Either of these two consequently causes a faster solidification rate. Figure 7 also shows that on the computed flows field, the inlet flow distribution has little influence on the solidification rate at the pipe exit for the specified parameters and the Reynolds number. As shown consistently in each set of constant Stefan number, the discrepancy of the solid-liquid interface between the slug flow and the computed exact flow increases as the solidification progresses. Similarly, Figure 8 depicts the effect of the Reynolds number on the progress of the solidification front for Sf = 0.643 and Pr = 13.2. It illustrates that at lower Reynolds number and

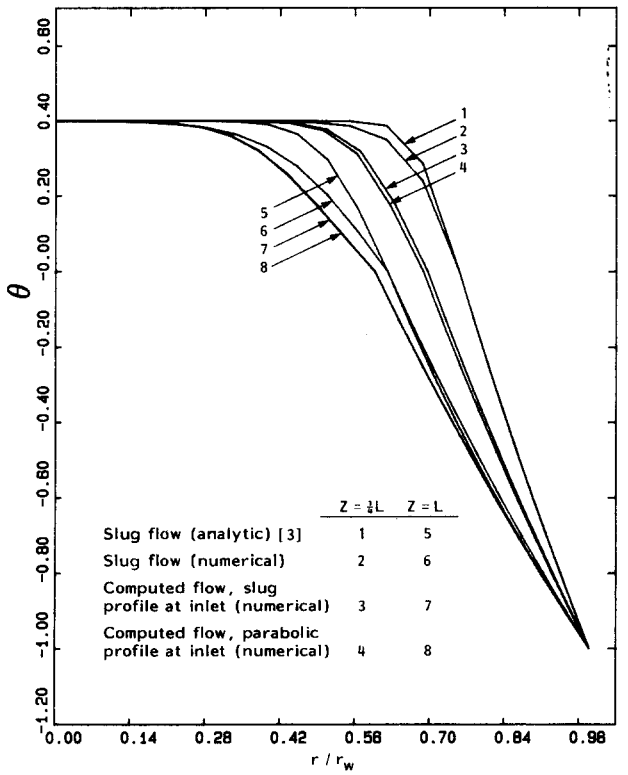

Figure 3 Temperature distribution in radial direction at $t=1$ h at selected axial locations for Sf=0.643, Pr=13.2, Re=100

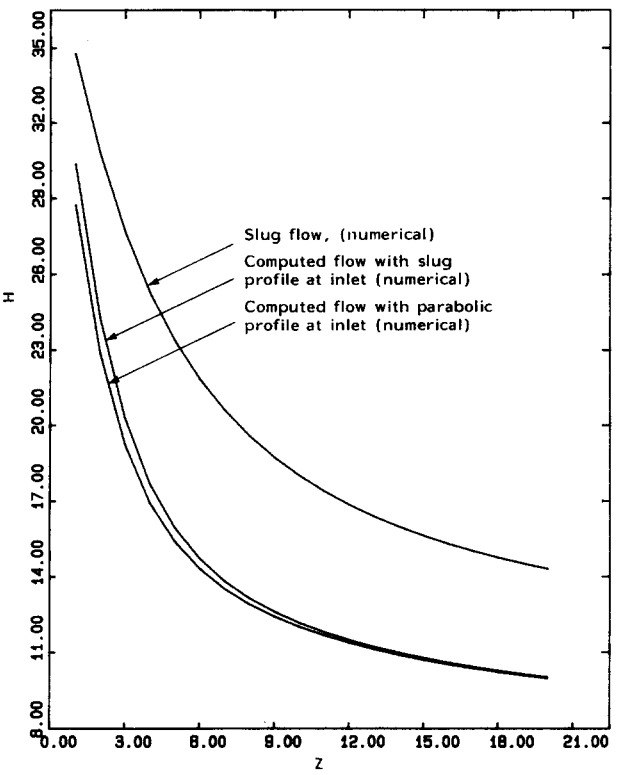

Figure 5 Variation of the local heat transfer coefficient at interface along the axial direction at $t=1$ h for Sf=0.643, Pr=13.2, Re=100

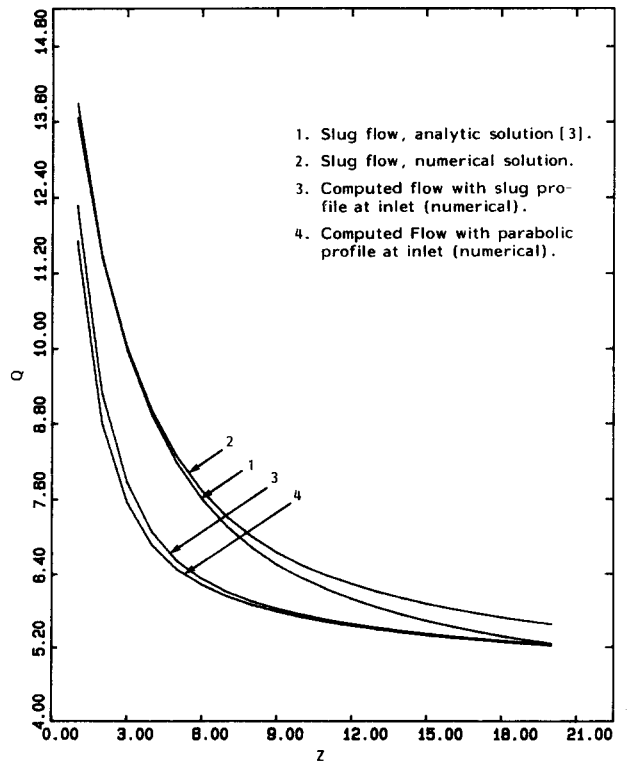

Figure 4 Local heat flux distribution along the wall of cylinder at $t=1$ h for Sf=0.643, Pr=13.2, Re=100

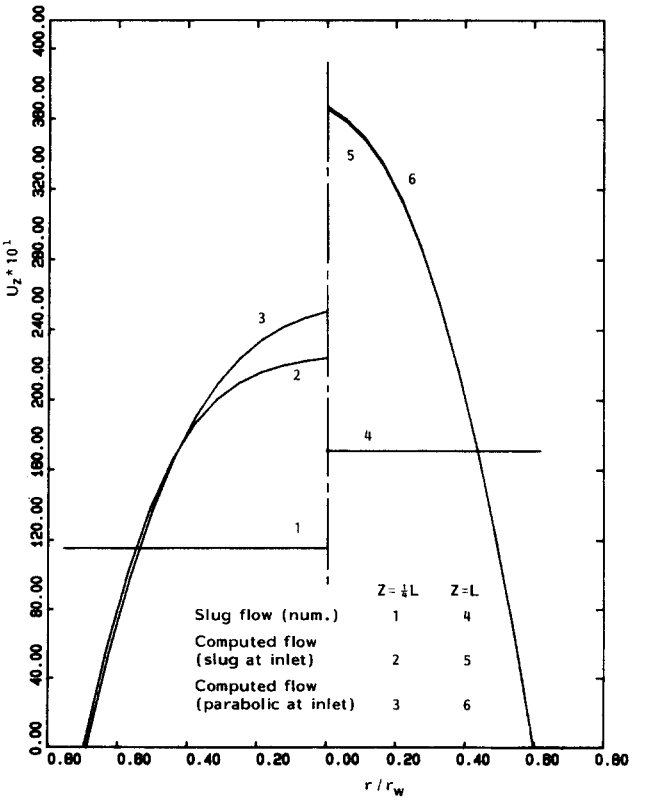

Figure 6 Velocity profiles (U_z) at selected axial locations for $t=1$ h for Sf=0.643, Pr=13.2, Re=100

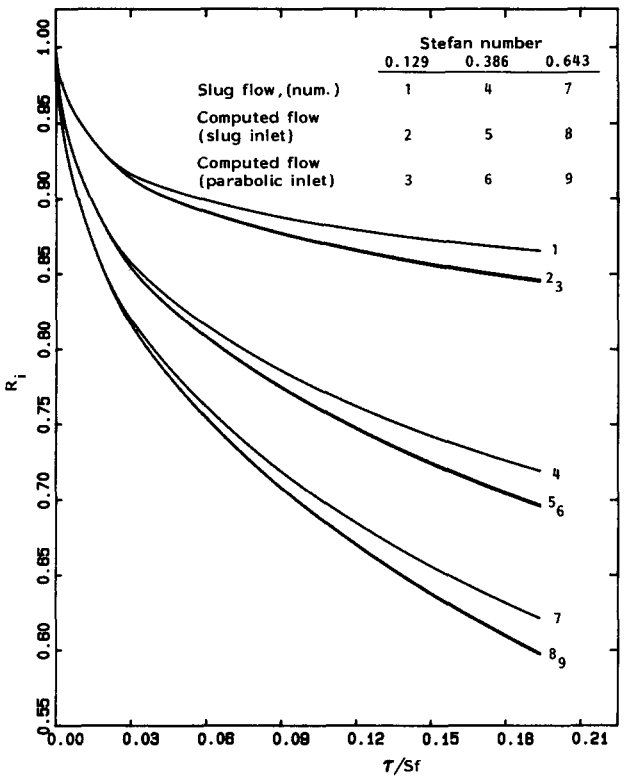

Figure 7 Effects of Stefan number on the location of solid-liquid interface at the exit of the problem domain for Pr=13.2, Re=100

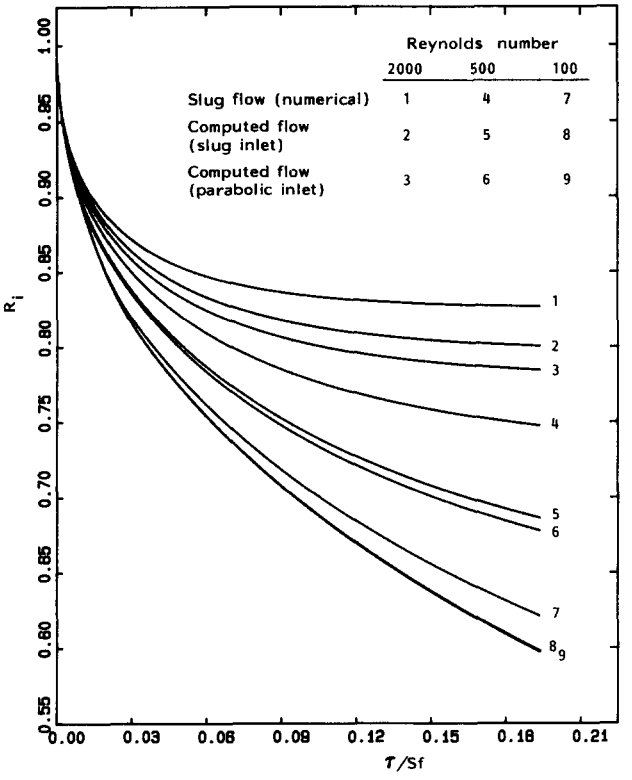

Figure 8 Effects of Reynolds number on the location of solid-liquid interface at the exit of the problem domain for Sf=0.643, Pr=13.2

smaller flow rate the solidification rate increases. This difference in the solidification rate at the pipe exit between the slug flow and the computed exact flow ranges from 3.9 to 10.3% when based on the radius of the solidification front, and ranges from 6 to 27.5% when based on the solidification thickness. It also shows that at lower Reynolds number, the effect of velocity profiles at the pipe inlet is less pronounced.

Additional results and a detailed analysis of the numerical scheme are presented in Ref. 26.

Conclusions

A numerical formulation of the coupled fluid flow–solidification problem for developing internal pipe flows is presented. The accuracy of the approach is demonstrated by comparing it with available solutions for slug flow and is found to be satisfactory. The Landau transformation utilized here shows that algebraic transformation techniques can be used effectively for this and other problems of similar geometries; however, advanced numerical techniques, such as numerical grid generation methods, have to be employed for more complex geometries, although with substantial increase in computational time. It is found that the influence of the flow velocity distribution on the solidification rate cannot be ignored, and the velocity distribution should be solved simultaneously with the temperature distribution. One of the primary advantages of the present approach is the flexibility in the boundary conditions; pipe wall temperature can be varied arbitrarily in the axial direction, and different flow distributions can be considered at the inlet of the pipe without necessitating any major change in the computational procedure. The present method is computationally feasible, with a CPU time of approximately 0.450 s for the slug velocity profile and 0.675 s for the varying velocity profile per computational cycle on a VAX 11/780 computer.

References

1 Hirschberg, H. G. Freezing of piping systems. *Kaltetechnik* 1962, **14**, 314–321

2 Zerkle, R. D. and Sunderland, J. E. The effect of liquid solidification in a tube upon the laminar-flow heat transfer and pressure drop. *J. Heat Transfer* 1968, **90**, 183–190

3 Ozisik, M. N. and Mulligan, J. C. Transient freezing of liquids in forced flow inside circular tubes. *J. Heat Transfer* 1969, **91**, 385–390

4 Sadeghipour, M. S., Ozisik, M. N., and Mulligan, J. C. Transient freezing of a liquid in a convectively cooled tube. *J. Heat Transfer* 1982, **104**, 316–322

5 Shibani, A. A. and Ozisik, M. N. Freezing of liquids in turbulent flow inside tubes. *Can. J. Chem. Eng.* 1977, **55**, 672–677

6 Shibani, A. A. and Ozisik, M. N. A solution of freezing of liquids of low Prandtl number in turbulent flow between parallel plates. *J. Heat Transfer* 1977, **99**, 20–24

7 Bilenas, J. A. and Jiji, L. M. Variational solution of axisymmetric fluid flow in tubes with surface solidification. *J. Franklin Inst.* 1970, **289**, 265–279

8 Gilpin, R. R. The morphology of ice structure in a pipe at or near transient Reynolds numbers. Heat Transfer—San Diego 1979, AIChE Symposium Series 189, Vol. 75, pp. 89–94

9 Gilpin, R. R. Ice formation in a pipe containing flows in the transition and turbulent regimes. *J. Heat Transfer* 1981, **103**, 363–368

10 Seki, N., Fukusako, S., and Younan, G. W. Ice-formation phenomena for water flow between two cooled parallel plates. *J. Heat Transfer* 1984, **106**, 498–505

11 Cheung, F. B. and Epstein, M. Solidification and melting in fluid flow. In *Advances in Transport Processes*, Vol. 3, Wiley, New York, 1984

12 Barakat, H. Z. and Clark, J. A. Analytical and experimental study of the transient laminar natural con containers. *ASME and AICE* 1966, **2**, 152–162
13 Kroeger, P. G. and Ostrach, S. The solution of a two dimensional freezing problem including convection effects in the liquid region. *Int. J. Heat Mass Transfer* 1974, **17**, 1191–1207
14 Yim, A., Epstein, M., Bankoff, S. G., Lambert, G. A., and Hauser, G. M. Freezing-melting heat transfer in a tube flow. *Int. J. Heat Mass Transfer* 1978, **21**, 1185–1196
15 Petrie, D. J., Linehan, J. H., Epstein, M., Lambert, G. A., and Stachyra, L. J. Solidification in two-phase flow. *J. Heat Transfer* 1980, **102**, 784–785
16 Thomason, S. B. and Mulligan, J. C. Experimental observations of flow instability during turbulent flow freezing in a horizontal tube. *J. Heat Transfer* 1980, **102**, 782–784
17 Thomason, S. B., Mulligan, J. C., and Everhart, J. The effect of internal solidification on turbulent flow heat transfer and pressure drop in a horizontal tube. *J. Heat Transfer* 1978, **100**, 387–396
18 Sparrow, E. M., Patankar, S. V., and Ramadhyani, S. Analysis of melting in the presence of natural convection in the melt region. *J. Heat Transfer* 1977, **99**, 520–526
19 Moore, F. E. and Bayazitoglu, Y. Melting within a spherical enclosure. *J. Heat Transfer* 1982, **104**, 19–23
20 Saitoh, T. and Hirose, K. High Rayleigh number solutions to problems of latent heat thermal energy storage in a horizontal cylinder capsule. *J. Heat Transfer* 1982, **104**, 545–553
21 Gupta, R. S. and Kumar, A. Treatment of multi-dimensional moving boundary problems by coordinate transformation. *Int. J. Heat Mass Transfer* 1985, **28**, 1355–1366
22 Rieger, H., Projahn, U., and Beer, H. Analysis of the heat transport mechanisms during melting around a horizontal circular cylinder. *Int. J. Heat Mass Transfer* 1982, **25**, 137–147
23 Yost, B. A. The analysis of fluid flow/solidification problems in arbitrarily shaped domains. Ph.D. Thesis, University of Delaware, Newark, 1984
24 Uchikawa, S. and Takeda, R. Use of a boundary-fitted coordinate transformation for unsteady heat conduction problems in multiconnected regions with arbitrarily shaped boundaries. *J. Heat Transfer* 1985, **107**, 494–498
25 Roache, P. J. *Computational Fluid Dynamics*. Hermosa, 1982
26 Wei, S. S. and Guceri, S. I. Numerical investigation of solidification in internal pipe flows. George W. Laird Computer-Aided Engineering Laboratory, CAE Report-5/1984 Department of Mechanical and Aerospace Engineering, University of Delaware